Correlation between ignition delay time and cetane number of Diesel fuel using a shock tube

Claudio Marcio Santana
Universidade Federal de Ouro Preto

RESUMO

The ignition delay time and cetane number of the fuel are important thermal properties that influence the quality of the combustion process in compression ignition engines. The higher the cetane number of the fuel, the shorter the ignition delay time and the better the combustion quality. The objective of this work was to measure the ignition delay time of diesel fuel using a shock tube, develop a computational routine to predict and characterize the delay time in the shock tube and compare these experimentally measured and simulated times with the cetane number of the respective fuel. The results showed good approximation between the experimental results and numerical simulation. The ignition delay times found in the experimental tests ranged from 316 to 856μs. The ignition delay times found in the numerical simulations under the same operating conditions as the experimental tests ranged from 425 to 1120μs. This work is relevant because it was able to characterize the ignition delay time through numerical simulation in the same order of magnitude found in the experimental tests in the shock tube.

INRODUCTION

In an effort to improve the energy efficiency extracted from the combustion of fuels and to reduce the emissions produced by this combustion, research related to the development and implementation of new technologies for the study of combustion has been carried out. These studies involve the determination and characterization of parameters related to the fuel ignition process. The ignition of the fuel-air mixture can be quantified by the following parameters: ignition delay time, shock wave pressure, flame temperature, density of the mixture of combustion products, chemical reaction speed, shock wave propagation speed and energy released in the combustion process. In computational simulation works, the use of meshes is important in terms of the precision achieved in the computationally simulated results with experimental tests. Meshes are simple geometric structures such as triangles or rectangles that serve as a model to characterize a given physical phenomenon. The choice of a mesh depends on computational performance factors and influences the simulation results. The larger the area covered by each mesh element, the fewer elements are needed to process the simulation and the faster the process will be. The smaller the elements of a mesh, the more accurate the simulation result will be, but with a higher computational cost. In this work was developed from a computational routine in the integrated Lazarus programming environment to simulate shock tube combustion parameters. Santana and Barros [1] defines the shock tube as an equipment used to study the shock waves movement under different temperature and pressure conditions, gas compressibility and fuel combustion. The equipment is constructed by a metal tube separated by a diaphragm, which divides the equipment into two sections. The high-pressure section is called the driver section while the low-pressure section is called the driven section. The diaphragm separating the two sections is designed to withstand a certain pressure, when that pressure is reached the diaphragm breaks and a compression wave is formed and moves towards the driven section. Instantly an expansion wave is formed and propagates towards the driver section. This movement of the gas mass inside the shock tube causes an increase in pressure and temperature in the driven section and a reduction in pressure and temperature in the driver section. Santana et al. [2] conducted experimental tests in shock tube to measure and compare ignition delay times of conventional diesel, additive ethanol and biodiesel from soybean oil. The results shows that the ignition delay time of additive ethanol was twice as large as the ignition delay time of conventional diesel and the ignition delay time of biodiesel from soybean oil was approximately three times greater than the ignition delay time of diesel. Santana et al. [3] conducted experimental tests in shock tube to correlate the ignition delay times of conventional diesel, additive ethanol and biodiesel from soybean oil with the cetane number of the respective fuels. The tests were performed under the following initial conditions: reflected shock wave temperature from 903 to 1260K, equivalence ratio 1 and reflected shock wave pressures of 24bar. For conventional Diesel were found ignition delay times ranging from 316 to 856μs. For additive ethanol were found ignition delay times ranging from 342 to 863μs and for biodiesel from soybean oil were found ignition delay times ranging from 640 to 1782 μs. Cancino et al. [4] measured and simulated the

ignition delay time of surrogate gasoline A comprised of ethanol, iso-octane, n-heptane and toluene (40%, 37.8%, 10.2% and 12% by liquid volume), surrogate gasoline B comprised of ethanol, iso-octane and n-heptane (69%, 17%, and 14% by liquid volume) and surrogate gasoline C comprised of iso-octane, n-heptane and toluene (20%, 62%, and 18% by liquid volume). The experimental tests were performed at high-pressure shock tube and the numerical simulations was performed used the CHEMKIN software through the on detailed chemical kinetic mechanisms. The experimental tests and numerical simulations were performed under the following conditions: temperatures from 690 to 1200 K and pressures at 10, 30 and 50bar. For surrogate gasoline A were found delay times ranging from 28 to 8731μs, for surrogate gasoline B were found delay times ranging from 120 to 6230μs and for surrogate gasoline C were found delay times ranging from 180 to 1060 μs. The simulations are compared to experimental ignition delay data from the literature and the results shows that the right trend but fails to capture absolute values of the ignition delay times, especially at low temperatures. All kinetics models overestimated the ignition delay times in relation to experimental tests. Niu et al. [5] measured and simulated the ignition delay time of n-heptane and n-butanol comprising the following mixtures (pure n-heptane, 80/20, 50/50, 20/80 and pure n-butanol). The experimental tests also were performed at heated high-pressure shock tube and the numerical simulations was performed used the CHEMKIN software tools (CHEMClean, CHEMDiffs and CHEMThermo). The experimental tests and numerical simulations were performed under the following conditions: temperatures from 1200 to 1500K, pressures at 2 and 10 atm and equivalence ratios of 0.5 and 1. The results shows good prediction between experimental tests and numerical simulations. Were found delay times ranging from 90 to 1230 μs for pure n-heptane, from 120 to 950 μs for pure n-butanol and from 30 to 1010 μs for mixture with n-heptane and n-butanol. Luan et al. [6] simulated the physical properties of flow inside the shock tube with a small nozzle in the end plate. The shock tube used for simulation consisted of a 3.66m in driver section, a 4.54m driven section with internal diameter of 10cm and a tiny nozzle is located at the end plate of the driver section. The nozzle has an opening angle of 70 degree and an angle of 90 degree inside the shock tube. The simulations were performed with the commercial code ANSYS Fluent. Pressure, density and temperature were investigated and the results show that this special shock-tube setup can be used to study high-temperature gas-phase chemical reactions with reasonable accuracy. Weber at al. [7] simulated the reflection of a normal shock wave from the end wall of shock tube. The two-dimensional channel has been numerically simulated to investigate the unsteady, viscous interaction aspects of shock bifurcation. The algorithm has been coupled to the viscous transport terms of the Navier-Stokes equations and the numerical simulations were performed on the CONNECTION MACHINE. The results indicated that the high level of shearing between the reversed flow and the lower wall leads to instability of the viscous layer and the large and small-scale vortices lead to complex flow patterns and the high-speed in inviscid flow was deflected over this region. Liang et al. [8] simulated the ignition delay time of surrogate gasoline primary reference fuels (PRF90) comprised of n-heptane and iso-octane (10% and 90% by liquid volume), surrogate gasoline toluene reference fuels (TRF1) comprised of n-heptane and toluene (35% and 65% by liquid volume) and surrogate gasoline toluene reference fuels (TRF2) comprised of n-heptane, iso-octane and toluene (17%, 69% and 14% by liquid volume). The numerical simulations were performed by applicability of the dynamic adaptive chemistry through the simulation of homogeneous charge compression ignition and shock tube ignition delay times. The numerical simulations were performed under the following conditions: temperatures from 840 to 1175 K and pressures at 10, 30 and 50bar. For surrogate gasoline (TRF1) were found delay times ranging from 554 to 11005μs and for surrogate gasoline (TRF2) were found delay times ranging from 171 to 2355μs. Haylett et al. [9] measured and simulated the ignition delay time of three large normal alkanes, n-decane, n-dodecane and n-hexadecane, one large methyl ester, methyl decanoate and several diesel fuels, with a range of cetane indices from 42 to 55. The experimental tests and numerical simulations were performed under the following conditions: temperatures from 838 to 1381 K and pressures at 1.71 to 8.63 atm, oxygen concentrations from 1 to 21% and equivalence ratios from 0.1 to 2. Were found delay times ranging from 114 to 12544μs. The simulations are compared to experimental ignition delay data and the results shows that the current measurements show significantly shorter ignition delay times for rich mixtures than the model predictions. Comandini et al. [10] measured and simulated the ignition delay time of styrene/O_2 mixtures in argon, one of the main stable intermediates from the oxidation of large alkylated aromatic hydrocarbons. The experimental tests were performed at shock tube and the numerical simulations was performed through the on detailed chemical kinetic model. Fikri et al. [11] also measured and simulated the ignition delay time of pure and blends of n-heptane, iso-octane, ethanol, toluene and di-isobutylene. The experimental tests were performed at high-pressure shock tube and the simulations was performed based on detailed chemical kinetic mechanisms. The experimental tests and numerical simulations were performed under the following conditions: temperatures from 690 to 1200K and pressures at 10, 30 and 50 bar and were found delay times ranging from 115 to 10100μs. Campbell et al. [12] also measured and simulated the ignition delay time in the shock tube of n-heptane under the following conditions: temperatures from 651 to 823K, pressures between 6.1 and 7.4 atm and equivalence ratio of 0.75. Were found delay times ranging from 1220 to 10600μs. Lam et al. [13] also measured and simulated the ignition delay time in the shock tube of propane under the following conditions: temperatures from 980 to 1400K, pressures at 6, 24 and 60atm and equivalence ratio of 0.5. Were found delay times ranging from 200 to 10000μs. Walton et al. [14] investigated the ignition delay time in the shock tube of methyl butanoate at temperatures from 985

K, equivalence ratio 0.3 and pressures at 10.2atm. Was found delay times ranging from 19630 to 24180μs.

METHODOLOGY

A computational routine was implemented in object-oriented Pascal language, using the integrated Lazarus environment for building the meshes. Were generated 1000 horizontal points, which correspond to the length of the shock tube driven section and 50 vertically points, which correspond to the radius of the shock tube cross section, generating a total of 50000 rectangular cells. The mesh reading started at the point (1,1), which corresponding to the first point on the lower left of the shock tube driven section and followed vertically through the side wall of tube to the point (1,50) which corresponds to the upper left of the shock tube driven section. The process of reading the mesh points continues in the following columns until the last column of the shock tube driven section. In the last column the mesh reading starts with the point (1000,1) and continues until the last point the mesh (1000,50) that corresponds to the upper right of shock tube. Each rectangular cell of the mesh was divided into two triangular cells totaling a mesh with 100000 triangular cells. The Figure 1 shows the driver and driven sections of the shock tube and the region area the shock tube for simulation.

Figure 1 - Driver and driven sections of the shock tube, as well as region area the shock tube for simulation.

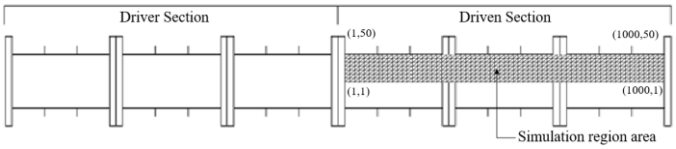

The driven section length and the cross-section radius of the shock tube measure, respectively 3000mm and 48.60mm. The Figure 2 shows the mesh dimensioning, the geometric parameters of driver and driven sections of the shock tube and the region area the shock tube for simulation.

Figure 2 - Driver and driven sections of the shock tube, as well as region area the shock tube for simulation.

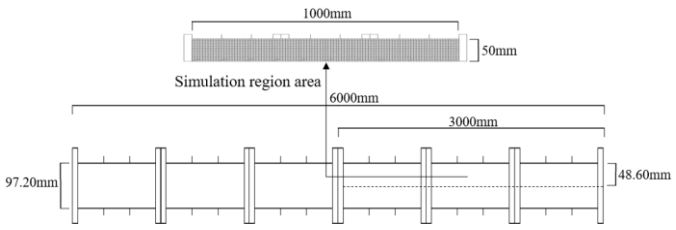

The total length of the driven section is 3000mm and the internal diameter is 97.20mm. For modeling and simulation, the upper half of the driven section was divided into four surfaces. Diaphragm surface, which corresponds the place where the mass flow from the driver section, which corresponds to the interval that originates in the horizontal symmetry line of the driven section and goes up to 48.60mm, which corresponds to half of the inner tube diameter. The shaft surface that corresponds to the shock tube symmetry line. The upper wall surface that corresponds to the upper wall of the shock tube driven section. The side wall surface that corresponds to the end wall of the shock tube driven section. The Figure 3 shows the unstructured triangular mesh generated in the Lazarus integrated environment, diaphragm, shaft, upper wall and side wall surfaces of the of the shock tube driven section used for simulation.

Figure 3 - Diaphragm, shaft, upper wall and side wall surfaces of the of the shock tube driven section.

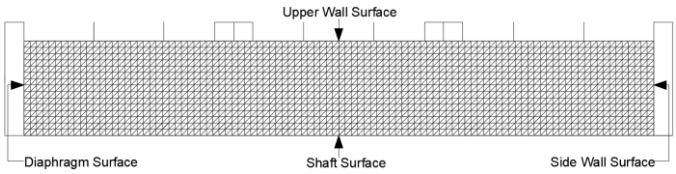

Each cell was identified according to the position occupied in the mesh. The cells that occupy the first column of the mesh, where the diaphragm ruptures (diaphragm surface), were called the diaphragm cells. Cells that are in contact with the (upper wall surface) of the tube were called upper wall cells, cells that are in the last column of the mesh and in contact with the end of the tube (side wall surface) were called the side wall cells, cells that are in contact with the shock tube symmetry line (shaft surface) were called shaft cells and the intermediates cells were called neighbors cells. The Figure 4 shows the position of the diaphragm, shaft, side walls, upper wall and neighbor's cells in the mesh.

Figure 4 - Position of diaphragm, side walls, shaft, upper wall and neighbor's cells in the mesh.

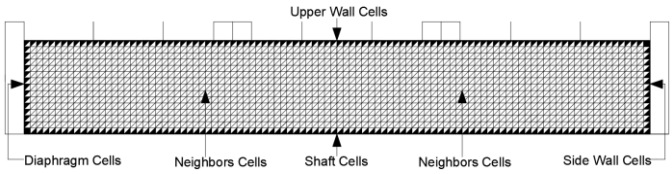

Cells called ghost cells were created on the diaphragm, shaft, upper wall and side wall surfaces to establish the boundary conditions necessary for simulation. The Figure 5 shows the position of the ghost cells in the mesh.

Figure 5 - Ghost cells in the mesh.

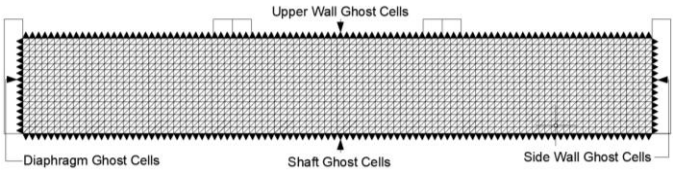

These cells are volumes of fictitious controls defined at the output of the computational domain of interest and which serve only for the implementation of boundary conditions.

The experiments were conducted in the heated shock tube facility of the Mobility Technology Center (CTM) of Federal University of Minas Gerais (UFMG). The experiments were carried out with the conventional diesel, which is the fuel normally distributed by the refineries to supply the fleet of trucks and buses and it has a cetane number of 43. The instrumentation within the shock tube used for the experiment included three pressure sensors (P1, P2 and P3), two temperature sensors (T3 and T1), a luminosity detection sensor (L1) and a fuel injector (FI). In the present work a mixture of the Nitrogen (N_2) and Argon (Ar) gases was used as the driver gas to obtain a longer test time. The Figure 6 shows the position of the sensors, fuel injector, aluminum diaphragm location and mixture of the Nitrogen and Argon inlet in the shock tube.

Figure 6 - Position of the sensors, fuel injector, aluminum diaphragm location and mixture of the Nitrogen and Argon inlet in the shock tube.

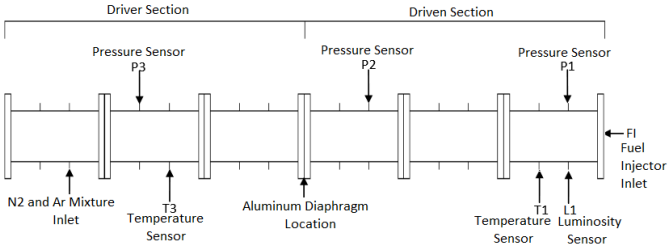

The pressure sensor P3 (located at 1700 mm before the aluminum diaphragm) was used to monitor the pressure in the driver section and the diaphragm rupture pressure. This piezoresistive sensor is the type TM25M produced by HYTRONIC. It has the following characteristics: Ability to measure relative or absolute pressure, measures pressure ranges: 0 to 350 bar with linearly proportional: 0 to 10V, operating temperature: 0 to 70ºC and response time: < 1ms. The pressure sensor P2 (located at 700 mm after the aluminum diaphragm) was used to indicates the moment of passage of the shock wave after diaphragm rupture. This information is used to control and define the fuel injection timing. This Piezoelectric pressure sensor is the type GU21 produced by AVL. This type of sensor was chosen to have adequate response time to capture the pressure variations within the of the tube. It has the following characteristics: Measuring range: 0 to 250 bars, load change rate: 1.5 mbar/ms, sensitivity: < 2% and uncertainty: ± 0.2 bar. The pressure sensor P1 (located at 2700 mm after the diaphragm) was used to indicates the moment of passage of shock in region 1 where combustion occurs. This sensor has the same characteristics that sensor P1. For monitor the temperature in the driver section was used an analog temperature sensor T3 type LM35 produced by TEXAS INSTRUMENTS. The main characteristics of the sensors are: calibrated in ºC, linear response with scaling factor of + 10mV/°C, accurate accuracy of 0.5ºC, measurement range: -55ºC to 150ºC, operation: 4V to 30V, self-heating less than 0.08ºC and non-linearity typical of ± 0.25ºC. For monitor and control the temperature in the driven section was used a temperature sensor T1 with the same characteristics that the temperature sensor T3 used in driver section. The luminosity detection sensor L1 was used to indicates the moment of combustion. This sensor consists of a light-sensitive photodiode, which has as its main characteristics: Luminosity detector with wavelength between 760 nm to 1100 nm, operating voltage: 1.3V to 5V and analog voltage output is inversely proportional to luminosity. At the moment of ignition, the voltage of this sensor decreases in function of flame in shock tube. This information together with the pressure signal of P1 sensor was used to calculated the ignition delay time. The fuel injector FI injects fuel into the shock tube when the sensor pressure P2 detects the passage of shock wave. The fuel injection pressure used in the tests was 300 bar. Under these conditions the injection time was adjusted for each type of fuel tested in order to maintain the stoichiometric ratio 1. The table 1 shows the accuracy of the sensors used in the experiments.

Table 1 - Accuracy of the sensors.

Sensors	Sensor type	Sensor accuracy
Pressure P3	TM25M	±0,25 bar
Pressure P1 and P2	GU21	± 0.20 bar
Temperature T1 and T3	LM35	0.50 °C

RESULTS AND DISCUSSION

The sensors P1 and L1 are in the same position in shock tube. The ignition delay time was calculated by the time difference between the passage of the shock wave by the P1 sensor and the start of the ignition detected by the luminosity detection sensor L1. The Table 2 listed the measured ignition delay time τ for conventional diesel. All measurements were carried out equivalence ratios 1. P2 and T2 represents the pressure and temperature of the incident shock wave, P5 and T5 represents the pressure and temperature of the reflected shock and τ is the ignition delay time measured. The experiments were performed in the temperature range of 903 to 1260K and target pressures were approximately 24 bar. Were found ignition delay times ranging from 316 to 856μs.

Table 2 - Measured ignition delay times for conventional diesel.

Incident shock		Reflected shock		Ignition delay time
P2 (bar)	T2 (K)	P5 (bar)	T5 (K)	τ (µs)
14.2	932	24.6	1150	362
14.2	945	24.3	1162	342
14	962	24.2	1260	329
13.7	874	23.6	940	603
14.2	912	23.8	1065	316
14.1	918	24.6	1082	418
13.9	915	23.1	980	443
13.4	902	24.2	1008	439
13.2	874	24.7	972	518
13.9	862	24.3	965	780
13.6	854	24.7	903	856
14	862	24.1	920	790
14.2	840	24.2	972	680
13.9	798	24.8	995	648
13.8	823	24.5	1040	490
13.6	890	23.8	1120	412
14	944	23.9	1243	325

The Figure 7 shows the linear regression of the experimental tests for conventional diesel, with an R^2 value of 0.95.

Figure 7 - Linear regression of the experimental tests for conventional diesel, with an R^2 value of 0.95.

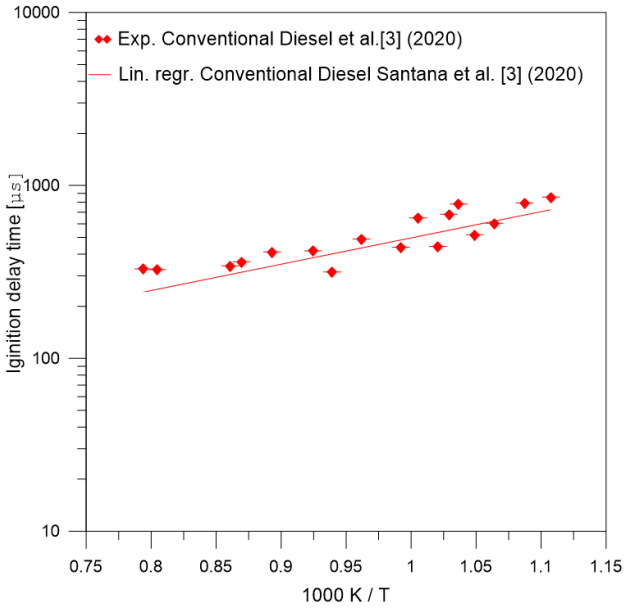

The Arrhenius equation obtained by the linear regression of the ignition delay times experimental tests for conventional diesel can be expressed by:

$$\tau_{Conv.\,dies.} = 0{,}24^{(-2{,}10)} \exp\left(\frac{3500}{T}\right).P^{(-0{,}09)} \qquad (1)$$

The Figure 8 shows the comparison of the ignition delay times simulated and the experimental tests with conventional diesel in the interval of 2 milliseconds. The experimental and simulation tests with conventional diesel were performed at reflected shock wave temperature of 1082K, equivalence ratio 1 and reflected shock wave pressures of 24 bar. The experimental measured and simulated ignition delay times were 418 and 515µs, respectively. The difference between the experimental and simulated test was 19%, this difference also can be explained by the measurement in the shock tube, that as already explained the ignition delay time was calculated by the time difference between the passage of the shock wave by the pressure sensor and the start of the ignition detected by the luminosity detection sensor.

Figure 8 - Comparison of the ignition delay times simulated and the experimental tests with conventional diesel in the interval of 2 milliseconds.

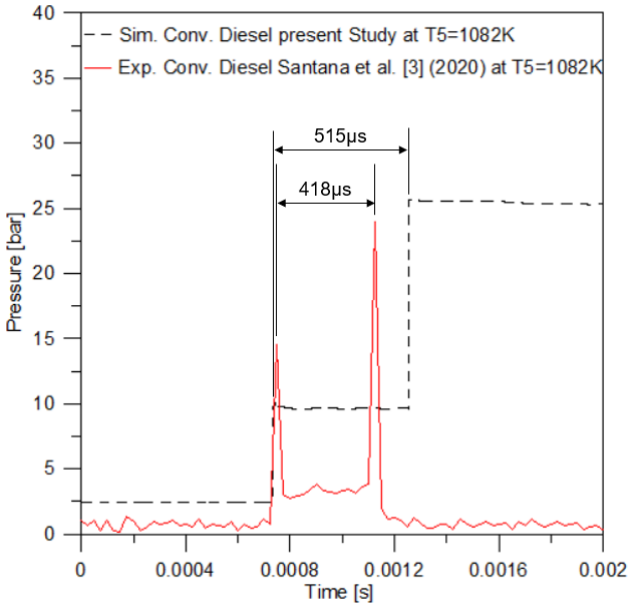

The table 3 listed the simulated ignition delay times for conventional diesel. Were performed 22 simulations and all measurements were carried out equivalence ratios 1, temperature ranged from 880 to 1300K and target pressures approximately 24 bar. The simulations were performed at previously defined temperatures according to the experimental tests performed and typical temperatures simulated by other authors. In these simulations were found times ranging from 425 to 1890µs.

Table 3 - Simulated ignition delay times for conventional diesel in present study.

Conventional diesel		
T5 (K)	P5 (bar)	τ (µs)
880	24.4	1890
900	24.4	1208
920	24.4	848
940	24.4	726
960	24.4	665
980	24.5	624
1000	24.4	590
1020	24.5	562
1040	24.6	532
1060	24.6	518
1082	24.6	515
1100	24.5	490
1120	24.5	481
1140	24.5	468
1160	24.5	452
1180	24.5	447
1200	24.6	440
1220	24.6	434
1240	24.5	430
1260	24.5	428
1280	24.6	427
1300	24.6	425

The figure 9 shows the comparison of the ignition delay times simulated in present study with the experimental tests with conventional diesel. All experiments were performed at reflected shock wave pressure of 24 bar and equivalence ratios of 1.

Figure 9 - Simulation and experimental results for conventional diesel.

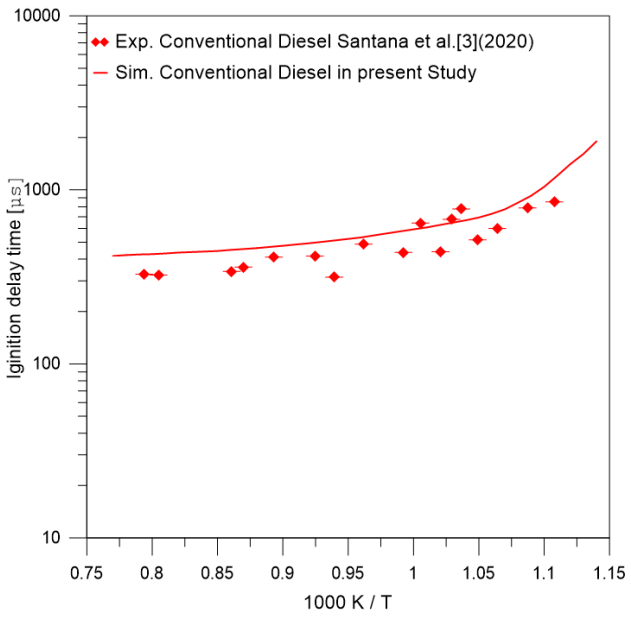

The simulation results in present study showed a good approximation of the experimental tests. The slope of the upward curves above 1.1 shows that, at low temperatures (< 910K) all fuel simulated had long ignition delay times. This simulation confirms that the ignition delay time increases with the reduction temperature and that thermal ignition does not occur at low temperatures. There was not occurrence of thermal ignition in the tests at temperatures below 910K. The slope of the downward curves below 0.82 shows that, at high temperatures (> 1220K) all fuel simulated had low ignition delay times and between 0.82 and 1.1, the simulation showed a linear increase in ignition time with temperature. As show, in all simulations the ignition delay times found were greater than in the experimental tests. Considering all temperature range, the difference between the experimental and simulated test was approximately 15%, this difference also can be explained by the measurement in the shock tube, that the ignition delay time was calculated by the time difference between the passage of the shock wave by the pressure sensor and the start of the ignition detected by the luminosity detection sensor.

CONCLUSIONS

The computational routine using Lazarus code compiler was developed to prediction and characterization ignition delay time, pressure, temperature generated and energy released in the combustion process of conventional diesel in a shock tube. The ignition delay times of conventional diesel simulated in this study are consistent with experimental tests performed and those found in the literature. For conventional diesel fuel were found times ranging from 425 to 1890µs. In general, at high-temperatures (> 1000K) the delay time varied significantly because the increase activation energy in this condition. At low-temperatures (< 1000K) this variation was more attenuated. This study also confirms the experimental tests, that the ignition time varies with increase pressure and temperature of the reflected shock. The results show good prediction between experimental tests and numerical simulations. Considering all temperature range, the difference between the experimental and simulated test was approximately 15%, this difference also can be explained by the measurement in the shock tube, that the ignition delay time was calculated by the time difference between the passage of the shock wave by the pressure sensor and the start of the ignition detected by the luminosity detection sensor. This work is relevant because it was developed computational routine in open software and the results achieved in the simulation were considered satisfactory, since they are in the same order of magnitude as the results found in the experimental tests carried out by Santana et al [3] and other works.

REFERENCES

1. Santana, C.M. and Barros, J. E. M., Shock Tube Combustion Analysis, Internal Combustion Engine Technology and Applications of Biodiesel Fuel (2021), ISBN: 978-1-83968-750-1, doi:10.5772/intechopen.96870.
2. Santana, C., Barros, J., Carvalho, M., and Alves de Almeida, Jr., H., Measuring and Comparing the

Ignition Delay Times of Diesel, Ethanol Additive and Biodiesel Using a Shock Tube, SAE Technical Paper 2015-01-0802, (2015), doi:10.4271/2015-01-0802.

3. Santana, C.M., Barros, J. E. M., Junior, H. A. A, Braga, J. O. and Neto, J. C. B., Measuring and comparing the ignition delay time of the reference diesel, conventional diesel, additive ethanol and biodiesel from soybean oil using a shock tube, Journal of the Brazilian Society of Mechanical Sciences and Engineering (2020) 42:102, doi:10.1007/s40430-020-2183-z.
4. Cancino, L. R., Fikri, M., Oliveira, A. A. M. and Shulz, C., Autoignition of gasoline surrogate mixtures at intermediate temperatures and high pressures: Experimental and numerical approaches, Proceeding of the Combustion institute, 32 (2009) 501-508, doi:10.1016/j.proci.2008.06.180.
5. Niu, S., Zhang, J., Zhang, Y., Tang, C., Jiang, X., Hu, E. and Huang, Z., Experimental and modeling study of the auto-ignition of n-heptane and n-butanol mixtures, Combustion and Flame 160 (2013) 31 – 39, doi:10.1016/j.combustflame.2012.09.006.
6. Luan, Y., Olzmann, M. and Magagnato, F., Simulation of a Shock Tube with a Small Exit Nozzle, Journal of Thermal Science Vol.27, No.1 (2018) 34 – 38, doi.org/10.1007/s11630-018-0981-8.
7. Weber, Y. S., Oran, E. S., Boris, J. P. and Anderson, J. D., The numerical simulation of shock bifurcation near the end wall of a shock tube, Physics of Fluids 7, 2475 (1995), doi.org/10.1063/1.868691.
8. Liang, L., Stevens, J. G., Raman, S. and Farrell, J. T., The use of dynamic adaptive chemistry in combustion simulation of gasoline surrogate fuels, Combustion and Flame 156 (2009) 1493–1502, doi: 10.1016/j.combustflame.2009.02.008.
9. Haylett, D. R., Davidson, D. F. and Hanson, R. K., Ignition delay times of low-vapor-pressure fuels measured using an aerosol shock tube, Combustion and Flame 159 (2012) 552–561, doi:10.1016/j.combustflame.2011.08.021.
10. Comandini, A., Pengloan, G., Abid, S. and Chaumeix. N., Experimental and modeling study of styrene oxidation in spherical reactor and shock tube, Combustion and Flame 173 (2016) 425 – 440, doi.org/10.1016/j.combustflame.2016.08.026.
11. Fikri, M., Herzler, J., Starke, R., Schulz, C., Roth, P. and Kalghatgi, G. T., **Autoignition of gasoline surrogates' mixtures at intermediate temperatures and high pressures**, Combustion and Flame 152 (2008) 276 – 281, doi:10.1016/j.combustflame.2007.07.010.
12. Campbell, M. F., Wang, S., Goldenstein, C. S., Spearrin, R. M., Tulgestke, A. M., Zaczek, L. T., Davidson, D. F. and Hanson, R. K., **Constrained reaction volume shock tube study of *n*-heptane oxidation: Ignition delay times and time-histories of multiple species and temperature,** Proceedings of the Combustion Institute 35 (2015) 231 – 239. doi:10.1016/j.proci.2014.05.001.
13. Lam, K. Y., Hong, Z., Davison, D. F. and Hanson, R. K., **Shock tube ignition delay time measurements in propane / O_2 / argon mixtures at near-constant-volume conditions,** Proceeding of the Combustion Institute 33 (2011) 251 – 258, doi:10.1016/j.proci.2010.06.131.
14. Walton, S. M., Karwat, D. M., Teini, P. D., Gorny, A. M. and Wooldridge, M. S., **Speciation studies of methyl butanoate ignition,** Fuel 90 (2011) 1796 – 1804, doi:10.1016/j.fuel.2011.01.028.

Contact Information

claudio.santana@ufopedu.br

Acknowledgments

Federal University of Ouro Preto, Department of Mechanical Engineering.

Federal University of Minas Gerais, Department of Mechanical Engineering.